

10-1999

A scintillating plastic fiber tracking detector for neutron and proton imaging and spectroscopy

James Ryan

University of New Hampshire

J.R. Macri

University of New Hampshire - Main Campus

M.L. McConnell

University of New Hampshire - Main Campus

Richard A. Messner

University of New Hampshire - Main Campus

Wenhui Li

University of New Hampshire - Main Campus

See next page for additional authors

Follow this and additional works at: <http://scholars.unh.edu/ssc>

 Part of the [Astrophysics and Astronomy Commons](#)

Recommended Citation

Ryan, J.M.; Macri, J.R.; McConnell, M.L.; Messner, R.A.; Li, W.; Cutlip, H.H.; Zheng, Q.; Castaneda, C.M.; Romero, J.L., "A scintillating plastic fiber tracking detector for neutron and proton imaging and spectroscopy," Nuclear Science Symposium, 1999. Conference Record. 1999 IEEE , vol.1, no., pp.483,488 vol.1, 1999

This Conference Proceeding is brought to you for free and open access by the Institute for the Study of Earth, Oceans, and Space (EOS) at University of New Hampshire Scholars' Repository. It has been accepted for inclusion in Space Science Center by an authorized administrator of University of New Hampshire Scholars' Repository. For more information, please contact nicole.hentz@unh.edu.

A scintillating plastic fiber tracking detector for neutron and proton imaging and spectroscopy

Rights

(c) 2000 EEE

Authors

James Ryan, J R. Macri, M L. McConnell, Richard A. Messner, Wenhui Li, Hansford H. Cutlip, Quihua Zheng, Carlos Castaneda, and Juan L. Romero

A Scintillating Plastic Fiber Tracking Detector for Neutron and Proton Imaging and Spectroscopy

James M. Ryan¹, John R. Macri¹, Mark L. McConnell¹, Richard A. Messner², Wenhui Li²,
Hansford H. Cutlip¹, Qihua Zheng¹, Carlos M. Castaneda³, Juan L. Romero³

¹Space Science Center, University of New Hampshire, Durham, NH 03824

²Dept. of Electrical Engineering, University of New Hampshire, Durham, NH 03824

³Crocker Nuclear Laboratory, University of California, Davis CA 95616

Abstract

We report the results of recent calibration data analysis of a prototype scintillating fiber tracking detector system designed to perform imaging, spectroscopy and particle identification on 20 to 250 MeV neutrons and protons. We present the neutron imaging concept and briefly review the detection principle and the prototype description. The prototype detector system records ionization track data on an event-by-event basis allowing event selection criteria to be used in the off-line analysis. Images of acrylic phantoms from the analysis of recent proton beam calibrations (14 to 65 MeV range) are presented as demonstrations of the particle identification, imaging and energy measurement capabilities. The measured position resolution is < 500 μm . The measured energy resolution ($\Delta E/E$, FWHM) is 14.2% at 35 MeV. An effective technique for track identification and data compression is presented.

The detection techniques employed can be applied to measurements in a variety of disciplines including solar and atmospheric physics, radiation therapy and nuclear materials monitoring. These applications are discussed briefly as are alternative detector configurations and future development plans.

I. INTRODUCTION AND MOTIVATION

Neutron telescopes based on double scatters are particularly effective in high background environments [1], [2]. The neutron telescope described here, known as SONTRAC, the SOLAR Neutron TRACking telescope, is under development to study the high energy processes associated with solar flares [3]. When high-energy charged particle reactions occur on the surface of the Sun, neutrons carry away information about the spectrum of ions that produced them and can be used as diagnostic measures of that spectrum [4].

A number of other applications for such a device have also been identified. In the earth's atmosphere neutrons above

10 MeV produce so-called soft error upsets in microcircuitry and they also present a radiation health hazard for personnel at high altitudes [5], [6], [7]. Neutron telescopes can accurately determine the properties of the neutron background. Neutron tracking detectors can also be employed to accurately locate nuclear materials (waste, spills).

The success of proton radiotherapy is based on the precision with which the dose is deposited in the tumor volume [8]. The tracking detector described here can be used to directly detect incident protons and precisely image the absorbing material to properly register a patient within the proton beam.

II. NEUTRON IMAGING CONCEPT

The detector measures the energy and direction of neutrons by detecting double neutron-proton scatters and recording images of the ionization tracks of the recoil protons in a densely packed bundle of scintillating plastic fibers stacked in orthogonal layers. The kinematics of the scatter are determined by tracking the recoil protons.

The double-scattering of a non-relativistic neutron in a solid block of plastic scintillator is illustrated in Figure 1. Neutrons interact in plastic scintillator either by elastically scattering from hydrogen (n-p) or by interacting with carbon (n-C). The n-p events are the most useful. For the non-relativistic case,

$$\sin^2 \phi_n = \cos^2 \phi_p = \frac{E_{p'}}{E_n + E_{p'}} = \frac{E_{p'}}{E_n} \quad (1)$$

where E_n is the incident neutron energy; E_n and $E_{p'}$ are the scattered neutron and photon energies, respectively; ϕ_n and ϕ_p are the neutron and proton scatter angles, respectively. The kinematics of nonrelativistic scattering further dictate that the scattered neutron and proton momenta are perpendicular to one another ($\phi_n + \phi_p = 90^\circ$).

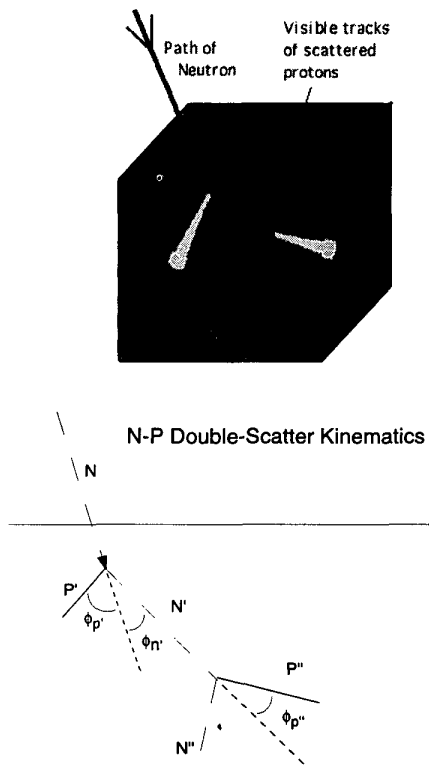


Figure 1: Schematic of non-relativistic double scatter neutron event in a block of plastic scintillator.

If the incident direction of a neutron is known, then the measurement of the energy and direction of a recoil proton in a single scatter is sufficient to determine the incident neutron energy. In particular, if the incident direction is known, then ϕ_n is determined and the neutron energy is

$$E_n = \frac{E_{p'}}{\cos^2 \phi_{p'}} \quad (2)$$

A more general approach, however, is provided by double-scatter events (Figure 1). If both recoil protons in a double scatter event are measured, then the energy and incident direction of the neutron are uniquely determined. The angular and energy resolution depend upon the ability to precisely measure the energy and direction of the recoil protons. Double scatter events can be used to measure neutron intensity from an extended source such as the secondary neutrons produced in the atmosphere by the primary cosmic radiation. For solar neutrons, double scatter events are also preferred, because they allow for a more complete separation of the source signal from the ambient background.

III. DETECTOR CONCEPT

The tracking detector concept is based on the use of a closely packed bundle of square cross section plastic-scintillator fibers. The fibers are arranged in stacked planes with the fibers in each plane orthogonal to those in the planes above and below. This alternating orientation allows one to record stereoscopic images and track ionizing particles in three dimensions in the scintillating fiber bundle. We have baselined 250 μm fibers on a 300 μm pitch. This size fiber was chosen so that a 10 MeV proton traverses several fibers before stopping. The neutron angular resolution is dependent upon the ability to precisely track the recoil protons. Track imaging employs two CCD cameras, one for each set of orthogonal fiber planes. The ionization track length is a sensitive measure of the recoil proton energy. The location of the Bragg peak, which corresponds to the greater ionization at the end of the track, fixes the track direction.

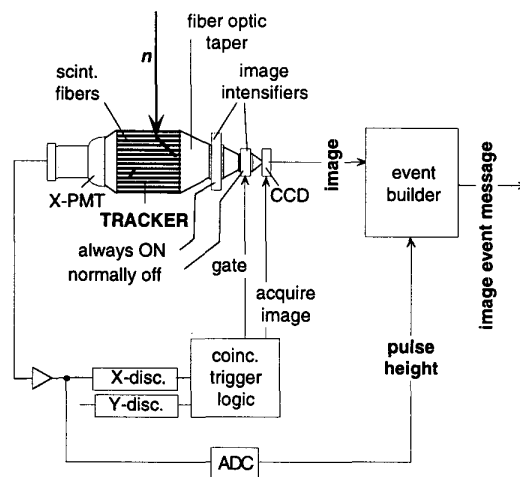


Figure 2: Functional diagram illustrating the detector concept and the signal processing logic.

A functional diagram of the readout scheme for an experiment utilizing the SONTRAC concept is shown in Fig. 2. The detector's spectroscopic, track detection, and imaging components cover the entire light emitting area of the scintillating fiber bundle and are duplicated in the orthogonal dimension (not shown). The scintillation light signal is collected and processed at both ends of the fiber bundle. At one end a signal above threshold from a photomultiplier tube (PMT) fires a discriminator that in turn provides a signal to the trigger logic circuitry. At the other end of the fiber bundle, fiber-optic tapers and a pair of image intensifiers demagnify, capture, and hold the scintillation-light image of the ionization track(s) for readout by the CCD camera. The first image intensifier in this chain is always ON. Its phosphor holds the

image for approximately 1 ms. The second image intensifier in this chain is normally in the gated-OFF condition and no image signal is passed to the CCD sensor. However, when the trigger logic registers the proper coincidence, the track image and PMT pulse height data are acquired and passed to an event builder and combined with auxiliary information for subsequent event-by-event analysis. For a fully 3-d implementation of the SONTRAC concept, this readout scheme would be applied in two orthogonal directions. This would provide the necessary information for reconstructing 3-d proton tracks.

For laboratory testing we have assembled a 2-d prototype. The prototype tracker is a 10 cm long bundle of 250 μm square scintillating plastic fibers on 300 μm pitch within a 12.7 mm (42 fiber) square envelope. Event readout in one direction limits tracking to 2-dimensions. The specifications of its key components and the manner in which it is operated (fiber composition and pitch, photocathode and phosphor composition, self triggered image gating and acquisition scheme) have been previously reported [9].

IV. NUCLEON MEASUREMENTS

The SONTRAC prototype was exposed to 14 MeV neutrons at San Diego State University and to higher energy (up to 65 MeV) neutrons and protons at the Crocker Laboratory cyclotron facility at the University of California at Davis. Figure 3 shows a raw CCD image of a neutron double interaction in the prototype fiber bundle. Two recoil proton tracks are evident from a single neutron (~65 MeV) incident from the top of the figure. Note the evidence of the Bragg peak. Gaps in the track images represent the passage of the ionizing particles through the passive cladding and EMA materials which surround each fiber.

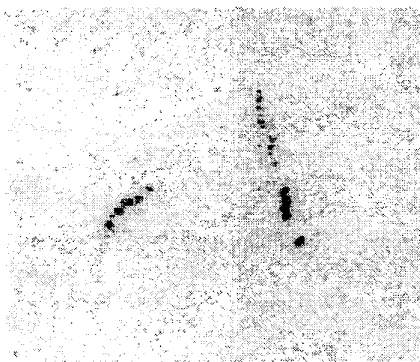


Figure 3. Raw CCD image of a double scatter from a ~65 MeV neutron incident from the top.

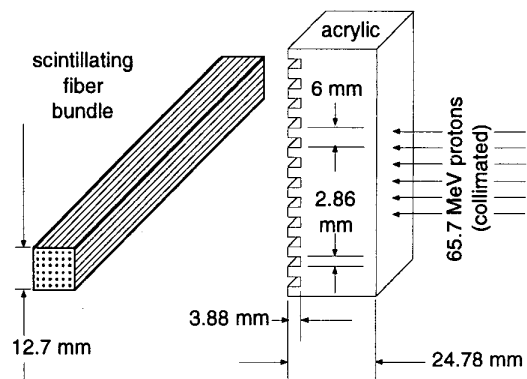


Figure 4: Test geometry for phantom imaging.

Measurements performed at the Crocker Laboratory used a variety of phantom absorbers placed between the proton beam and the tracking detector to measure and calibrate the response and to demonstrate its spectroscopic and imaging capabilities. The geometry for one such test is illustrated in Figure 4. The phantom absorber is a 24.78 mm thick acrylic block (1.18 g/cm^3) with 3.88 mm deep, 2.86 mm wide slots on 6 mm centers. The slots run parallel to the scintillating fiber axis. The prototype's scintillating fiber bundle spans slightly more than two pitch lengths of the phantom pattern.

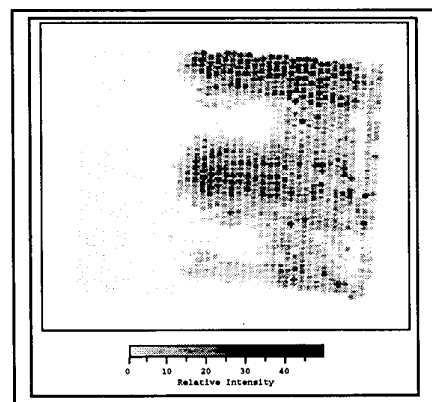


Figure 5. Image of slotted phantom accumulated from proton track images. Protons are incident from the right.

Figure 5 shows the accumulated sum of intensity per fiber for the track images of 555 selected events. Data are recorded for every event, thus permitting analysis on a variety of criteria. In this case, particles scattered from nearby material in the laboratory were identified and rejected either by the oblique slope of the track image or by the point of entry into the fiber bundle. The figure illustrates the signature of two pitch cycles of the phantom slot pattern.

V. TRACK RECOGNITION AND DATA COMPRESSION

The operation of SONTRAC represents the accumulation of large volumes of (imaging) data. For remote operations, much of the processing should take place on-board so as to reduce telemetry and/or data recording requirements. We have therefore been developing and evaluating data processing algorithms for (three-dimensional) event recognition, track recognition, data compression and track reconstruction that could be employed in future instrumentation. One such approach involves Hough Transforms. [10], [11].

Hough transforms allow us to extract information regarding the track orientation and relative strength (i.e., intensity) and, if we preserve enough of the full transform, the number of breaks in the colinear points that occur on the track.

The Hough transform collapses a line into a point and expands a point into a sinusoidal curve. For the Hough transform we describe a line segment with r and θ where r is the length of the normal from the origin to the line and θ is the angle between the normal and the x-axis (Figure 6). This transforms lines in "image space" to points in Hough space. An infinite number of straight lines can be drawn through any point in image space (such as a lit fiber). If the points in Hough space generated by the transformation of these lines are connected a sinusoidal curve is formed.

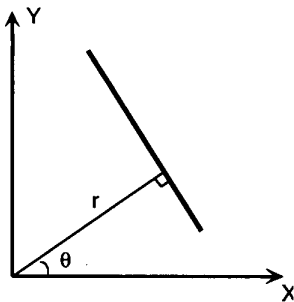


Figure 6: Hough transform definition of a line segment.

Figures 7a-7c show the Hough transform sequence, starting with a synthetic track like those that might be produced by SONTRAC. The track is horizontal and starts in the upper left hand corner of figure 7a. Each point along the track in image space becomes a sinusoidal curve in Hough space. If the track is extended to the left a normal line roughly 55 pixels long can be drawn. Since the track is horizontal the angle between the normal and the x-axis is roughly 90° . The Hough transform of the synthetic track is shown in Figure 7b, with the origin of the image at the top left. In this view, r is measured along the -y-axis running from 0 to 256 and θ is

measured along the x-axis from 0 to 180° . The sinusoidal curves intersect at a point corresponding to $\theta \approx 90^\circ$ and $r \approx 55$. The fact that there are two sets of curves with a phase difference between them tells us that there are two independent colinear line segments.

An inverse Hough transform has been coded and the Hough space in Figure 7b was "inverted" by this routine without deleting any data from the space (i.e., no data loss). The resulting image is shown in Figure 7c. In practice, one would likely perform some thresholding on the Hough transform to eliminate the ghosts seen in the bottom image.

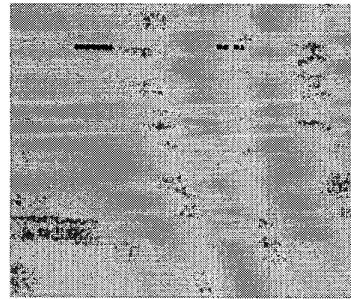


Figure 7a: Synthetic Proton track

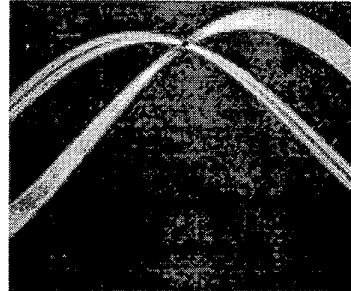


Figure 7b: Hough Transform of track

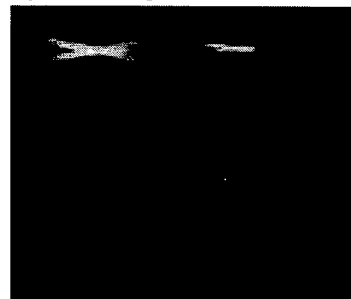


Figure 7c: Inverted Hough transform

With the Hough transform it may only be necessary to telemeter only a few pieces of information as opposed to a 250KB pixel image. Such data can be represented as a tuple of data such as θ , r , starting points, length, and intensity. The intensity measured along the particle track will be important

for discerning the Bragg peak, which is the region of increased ionization near the end of the particle's track.

Sample Hough transforms of real data are shown in Figures 8 and 9, using data taken from the SONTRAC prototype. A real proton ionization track from a 30 MeV neutron and its Hough transform are shown in Figure 8. Note the Bragg peak near the bottom of the track, indicating that the proton was traveling in the downward direction. As the tracks become longer the Hough signal becomes more compact. Figure 9 shows a true double-scatter event and its Hough

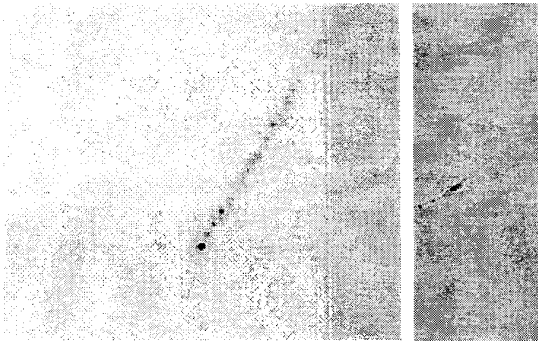


Figure 8: A proton ionization track as measured by the SONTRAC prototype (left) and its Hough transform (right).

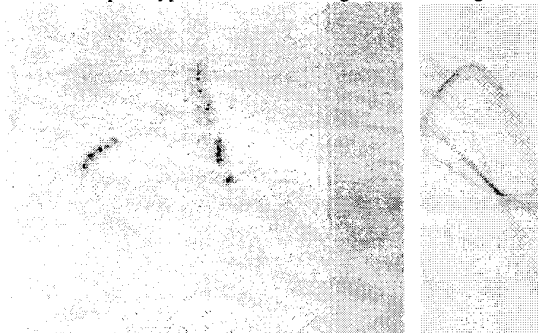


Figure 9: An n-p double scatter event as measured by the SONTRAC prototype (left) and its Hough transform (right).

transform. Here we see two distinct intensity peaks representing the two recoil protons that have different momentum vectors and displacements. Work needs to be done to quantify the starting point, the location of the Bragg peak and the track length. Some of this can be done with the 2-d prototype data.

A second compression technique capable of ~90% data reduction has been investigated. Once a track has been identified, only the relevant pixel data around the track and simple location and orientation data are recorded. These data can be telemetered to the ground where the tracks are reassembled and analysed.

VI. DEVELOPMENT OF APD READOUT TECHNOLOGY

We recently received funding from the NASA Explorer Technology program to develop a readout scheme for SONTRAC based on arrays of avalanche photodiodes (APDs). APD arrays represent a relatively new technology that may be well-suited to the readout of a SONTRAC fiber bundle. They have several unique features that make them very attractive for scintillating fiber readout. These include high quantum efficiency, low noise, compact design, low power requirements, and fast response. Furthermore, the APDs would have lower mass and occupy less volume than other readout technologies.

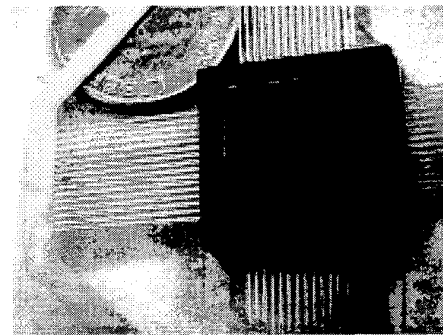


Figure 10: 64 element APD array with 1 mm² active area on a 1.27 mm pitch

We have been working closely with Radiation Monitoring Devices, Inc. (RMD), a major player in the development of APD technologies [12], [13]. They have succeeded in fabricating proportional mode APD arrays with active area pixel sizes less than 1 mm². The use of APD arrays to readout the individual scintillating fibers provides one signal per fiber. The SONTRAC design, with its 300 μm pitch, implies a large number of scintillating fibers. A fiber bundle that is 20 cm square, for example, would contain ~500,000 fibers. Furthermore, these signals must be processed and incorporated into trigger logic that is used to initiate the readout of a valid event. This problem is comparable to that faced by the FiberGLAST project (a version of the Gamma-ray Large Area Space Telescope based on scintillating fibers and being developed by a collaboration that includes UNH). The large number of channels and the complexity of these functions (signal processing, trigger generation and event readout) presents a formidable task, requiring some type of application-specific integrated circuit (ASIC). The goal of our two year Explorer Technology program is to demonstrate the feasibility of using APD arrays to read out a SONTRAC bundle and to

develop the associated front-end electronics that would be used in a SONTRAC instrument.

VII. FUTURE WORK

On-going work involves the fabrication and test of a three-dimensional SONTRAC science model (SM). Unlike the first SONTRAC prototype described above, the science model is based on a fiber bundle with orthogonal fiber layers, thus permitting track imaging and reconstruction in 3 dimensions. The SM will employ a $5 \times 5 \times 5$ cm scintillating plastic fiber tracking detector with appropriately sized optoelectronic components. The larger size of the SM fiber bundle will permit measurements at higher energies where n-C scatters occur. The goals of this science model study are to characterize the performance of the three dimensional version of SONTRAC and to refine the necessary electronics configuration and data processing algorithms for an engineering model. Calibrations are planned for both neutrons and protons at energies from 10-80 MeV, a range which covers from below the nominal threshold up to energies where neutron double scatter events are no longer contained within the SM fiber block.

VIII. CONCLUSIONS

Event-by-event detection and measurement of track length (energy), track direction and particle type has been accomplished. Specifically, we have fabricated a small SONTRAC prototype and demonstrated a self-triggered detector system for ionization track imaging of individual events. This has been done for minimum ionizing cosmic ray muons, the recoil protons from incident 14 MeV to 65 MeV neutrons and for incident 20 MeV to 65 MeV protons. We have demonstrated SONTRAC's neutron detection, spectroscopic and imaging capabilities from the threshold necessary for the solar physics study. We have explored and developed useful calibration and data analysis techniques using proton beams and in the process we have demonstrated imaging capabilities directly applicable to other fields. As a result of this effort key engineering parameters such as photoelectron yield, achievable energy threshold, scintillating fiber composition, fiber pitch, EMA requirements, photocathode and phosphor selection have been determined allowing us now to extend these techniques to larger detectors for higher energies with the ability to track in three dimensions.

IX. REFERENCES

- [1] G.Kanbach, et al., *J. Geophys. Res.*, vol. 79, p 5159, 1974.
- [2] J. M. Ryan, et al., in *Data Analysis in Astronomy IV*, p 261, Plenum Press, NY, 1992.
- [3] C. B. Wunderer, D. Holslin, J. R. Macri, M. L. McConnell, J. M. Ryan, "SONTRAC - A Low Background, Large Area Solar Neutron Spectrometer," *Workshop Record, Conference on the High Energy Radiation Background in Space, IEEE Nuclear and Space Radiation Effects Conference*, Snowmaass, Colorado, p 73, 1997
- [4] H. Hudson and J. Ryan. *Annual Review Astronomy and Astrophysics*, vol. 33, pp. 239-282, 1995.
- [5] M. Walt, *Introduction to Geomagnetically Trapped Radiation*, Cambridge University Press, 1994.
- [6] T. O'Gorman, et al., *IBM Journal of Research and Development*, vol. 40, No. 1, p. 41, 1996.
- [7] J. M. Ryan and R. Saxena, "Ground Level Neutron Measurements from 10-170 MeV", *Proc. Amer. Nucl. Soc. Topical Meetings. Radiation Protection and Shielding*, vol. 1, pp. 219-226, 1996.
- [8] J. L. Romero, et al., "Patient positioning for proton therapy using a proton range telescope", *Nuclear Instruments and Methods in Physics Research A*, vol. 356, pp. 558-565, 1995.
- [9] J. M. Ryan, J. Baltgalvis, D. Holslin, J. R. Macri, M. L. McConnell, A. Polichar, C. B. Wunderer, "A prototype for SONTRAC, a scintillating plastic fiber detector for solar neutron spectroscopy", *SPIE proceedings series*, vol. 3114 (1997 San Diego), pp. 514 - 525
- [10] R. O. Duda and P. E. Hart, *Commun. Ass. Comput. Mach.*, vol. 15, pp. 11-15, 1972.
- [11] J. Sklansky, "On the Hough Technique for Curve Detection," *IEEE Transactions on Computers*, vol. C-27, No. 10, Oct. 1978.
- [12] R. Farrell, et al., *Nucl. Instr. & Meth.*, A353, p. 176, 1994
- [13] M. Squillante, et al., *Proc. SPIE*, 2009, p. 64, 1993